

CERES Angular Distribution Model Working Group Report

Wenying Su

Wenying.Su-1@nasa.gov

NASA LaRC, Hampton VA

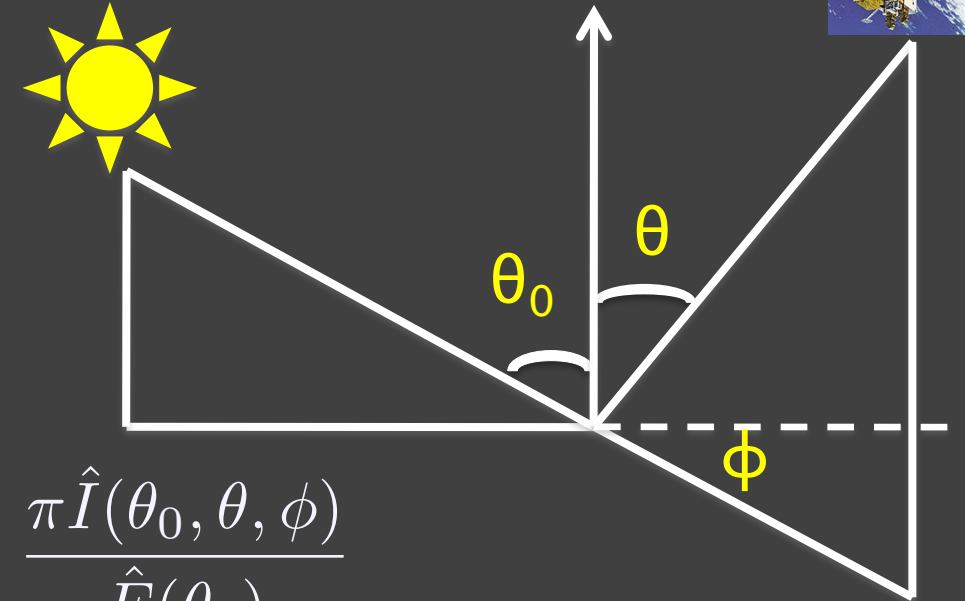
Lusheng Liang Zachary Eitzen Sergio Sejas

SSAI, Hampton VA

From radiance to flux: angular distribution models



- Sort observed radiances into angular bins over different scene types;
- Integrate radiance over all θ and ϕ to estimate the anisotropic factor for each scene type:



$$R(\theta_0, \theta, \phi) = \frac{\pi \hat{I}(\theta_0, \theta, \phi)}{\int_0^{2\pi} \int_0^{\frac{\pi}{2}} \hat{I}(\theta_0, \theta, \phi) \cos\theta \sin\theta d\theta d\phi} = \frac{\pi \hat{I}(\theta_0, \theta, \phi)}{\hat{F}(\theta_0)}$$

- For each radiance measurement, first determine the scene type, then apply scene type dependent anisotropic factor to observed radiance to derive TOA flux:

$$F(\theta_0) = \frac{\pi I_o(\theta_0, \theta, \phi)}{R(\theta_0, \theta, \phi)}$$

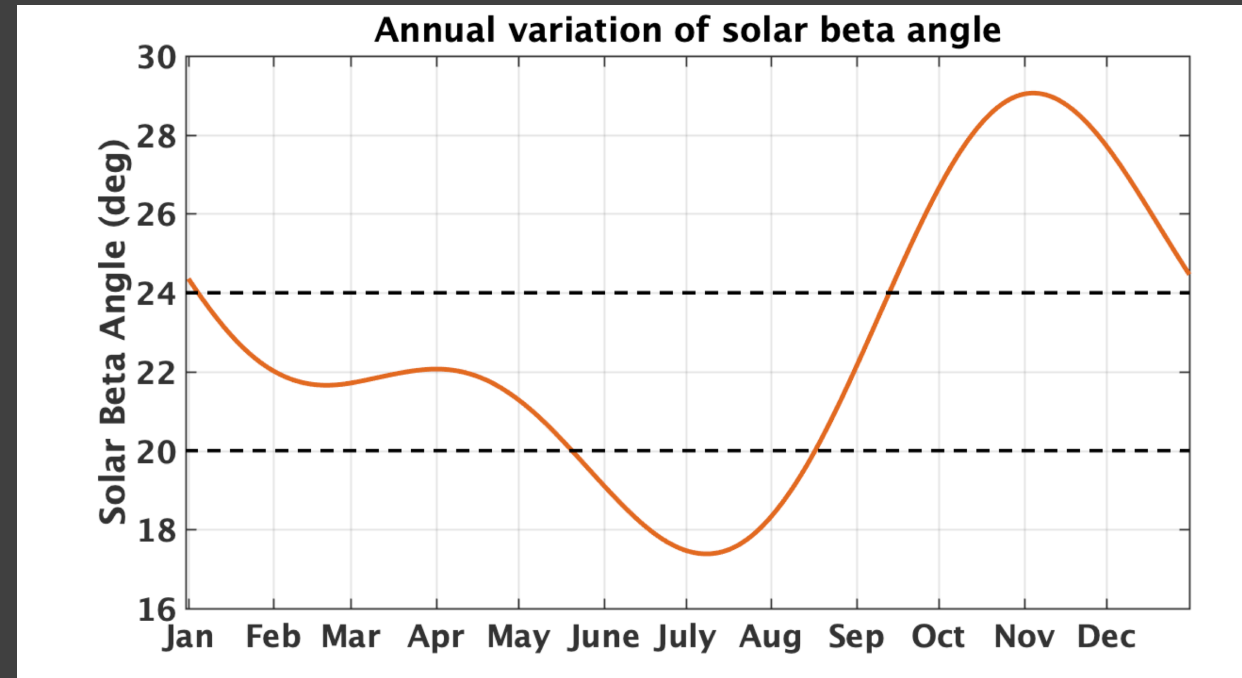


Outline

- CERES NPP SW ADMs and their impact on inverted fluxes
- Rearchitect the shortwave inversion code, with a focus on snow/ice scene identification
- Merged LW surface emissivity datasets for Ed5

NPP CERES ADMs

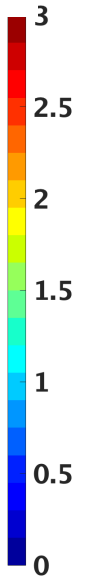
- NPP FM5 started to collect RAPS data in fall of 2019.
- CERES instrument on NPP is in restricted biaxial scan since March 24, 2020, to avoid viewing the spacecraft antenna, and to minimize the instrument degradation.
 - For solar beta angle $< 24^\circ$:
 - Clock angle: 25° — 169° , cone angle: 0° — 64°
 - Clock angle: 205° — 349° , cone angle: 0° — 64°
 - For solar beta angle $\geq 24^\circ$
 - Clock angle: 25° — 180° , cone angle 0° — 64°
 - Clock angle: 205° — 360° , cone angle 0° — 64°



Sample number comparison between NPP (20200324) and Aqua (20040324)

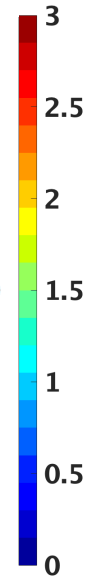
Aqua scan SZA : [20,30]

NPP scan SZA: [20,30]



Aqua scan SZA : [40,50]

NPP scan SZA: [40,50]



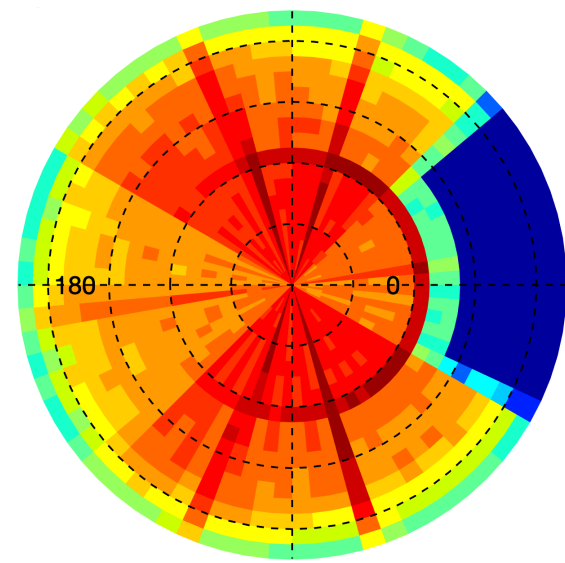
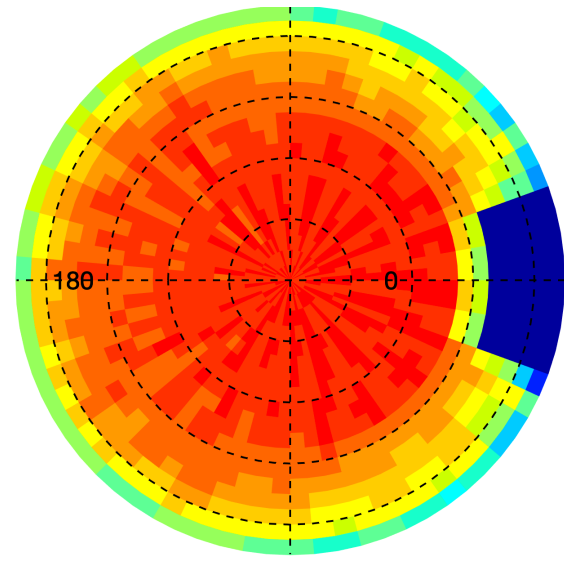
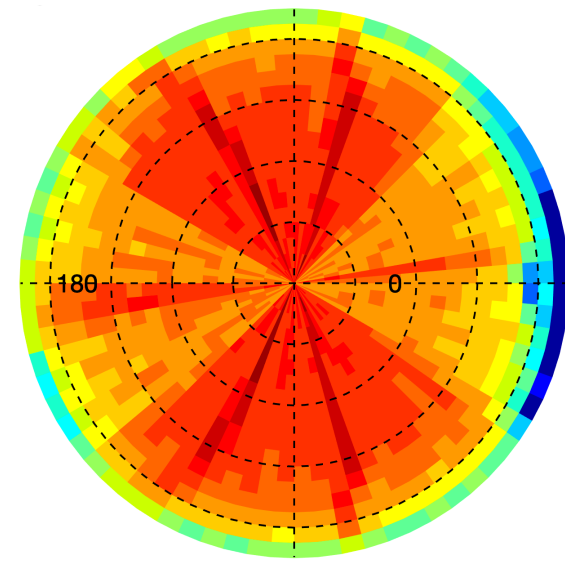
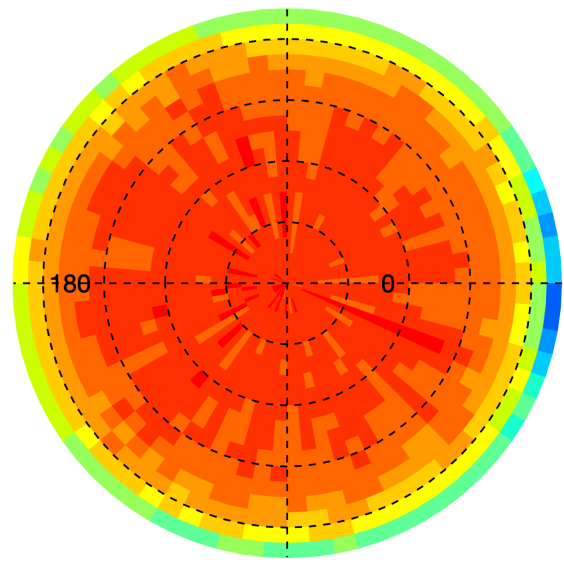
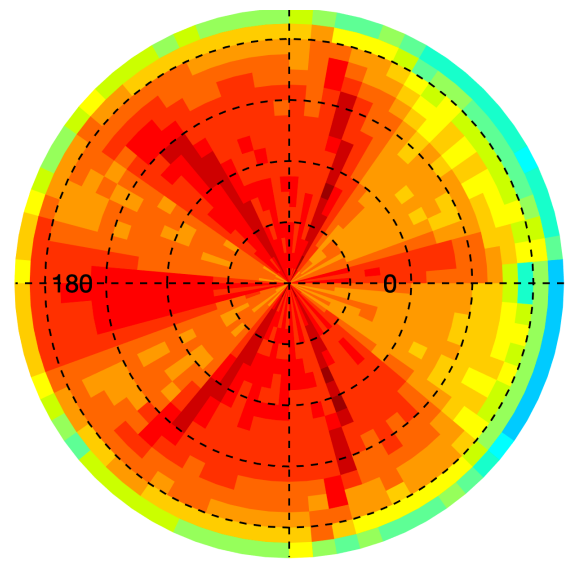
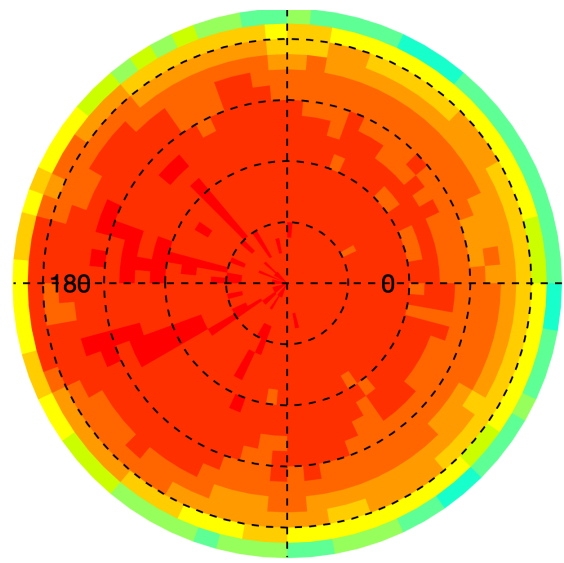
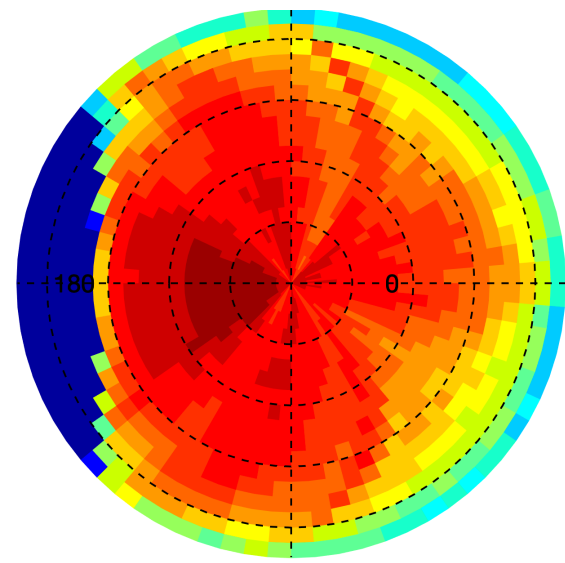
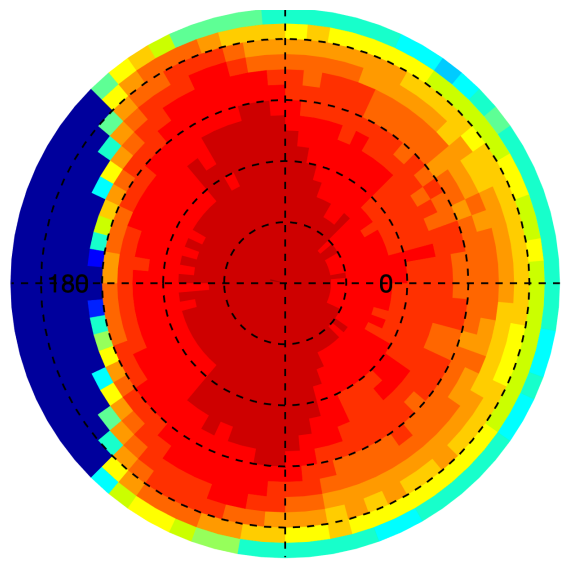
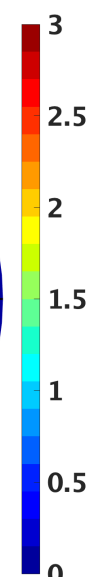
Aqua scan SZA : [60,70]

NPP scan SZA: [60,70]



Aqua scan SZA : [80,90]

NPP scan SZA: [80,90]

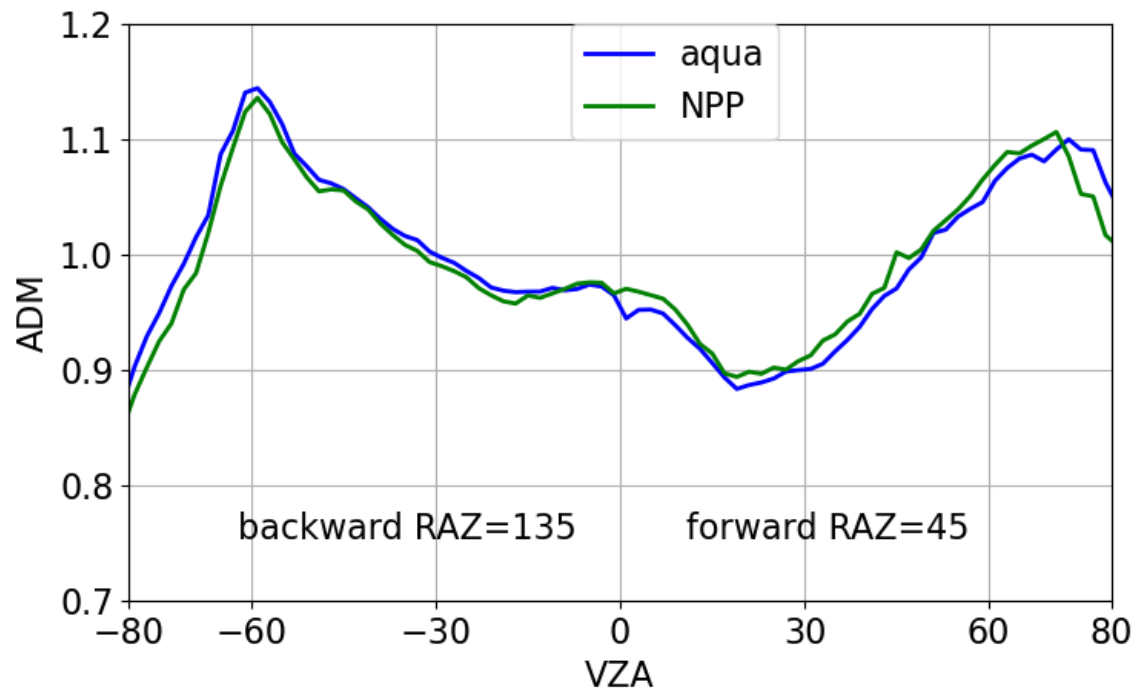


Developing NPP SW ADMs

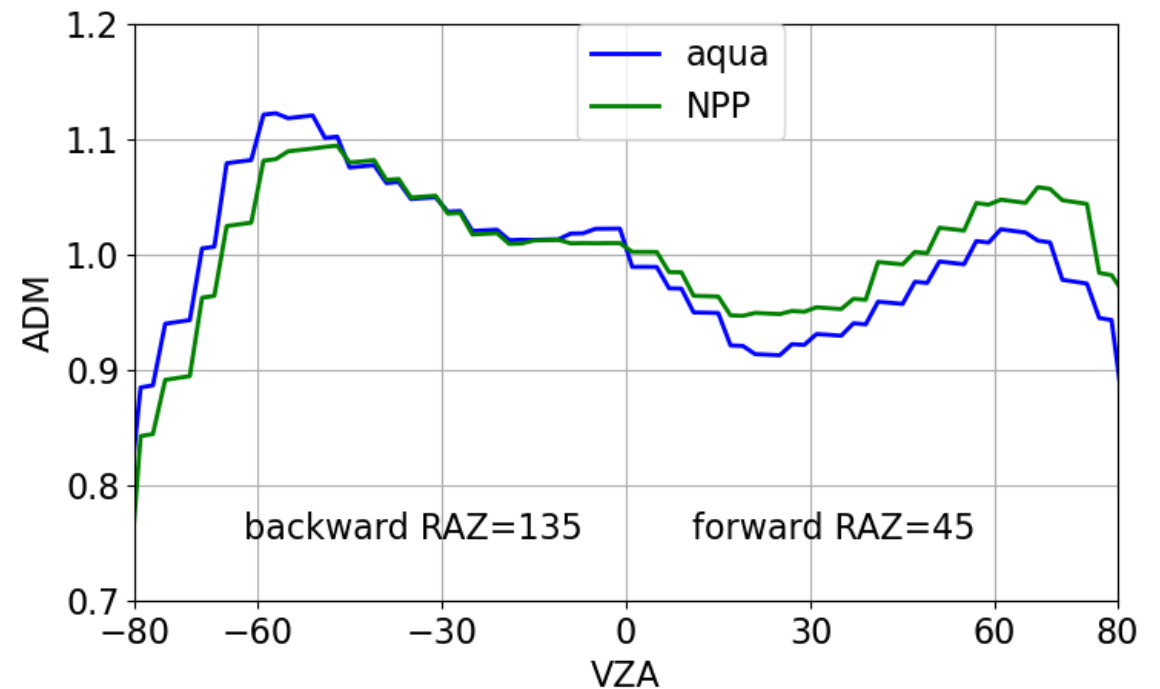
- Using NPP FM5 Ed2A data from 201610-202207 to develop SW NPP ADMs using the Ed4 Terra/Aqua methodology.
- NPP fluxes inverted using NPP ADMs are compared with fluxes in NPP Ed2A product that used Ed4 Aqua ADMs.

SZA=40° Overcast with cloud optical depth of 10

Ocean

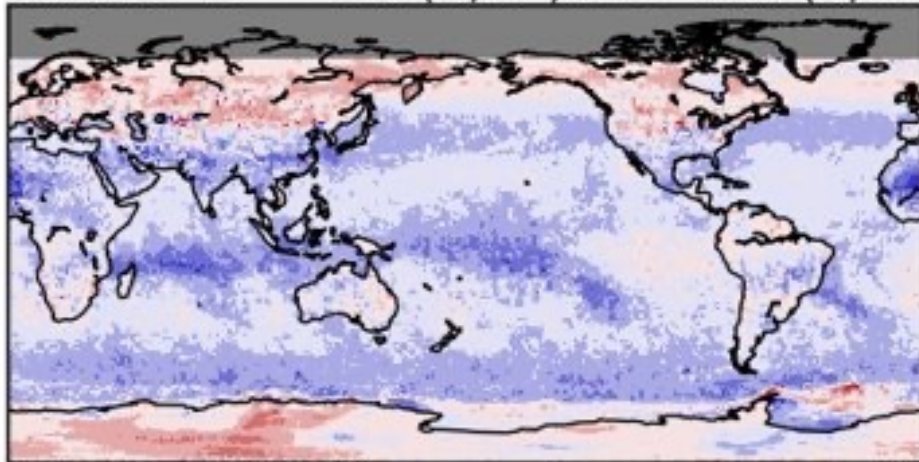


Land

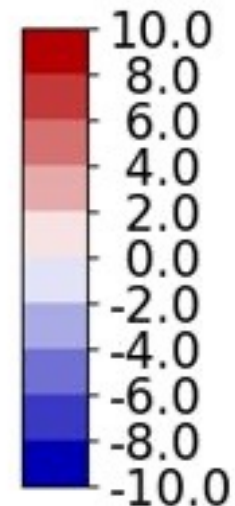
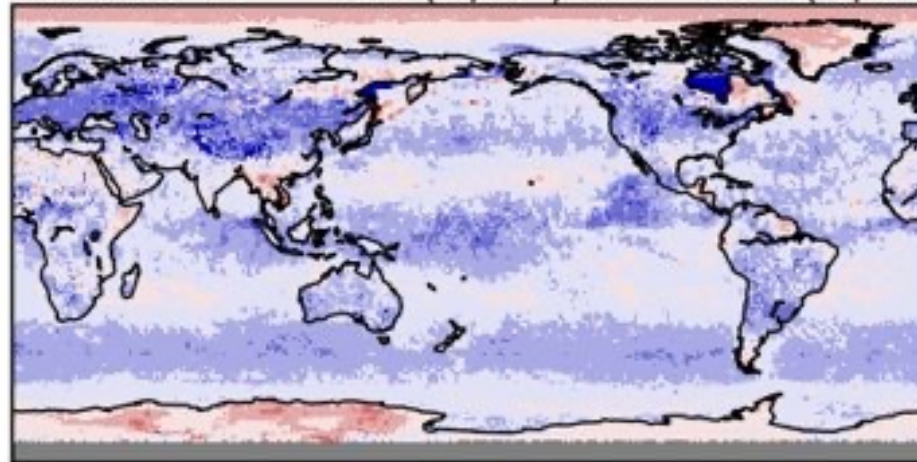


Instantaneous NPP flux difference due to ADMs: NPP ADM-Aqua ADM

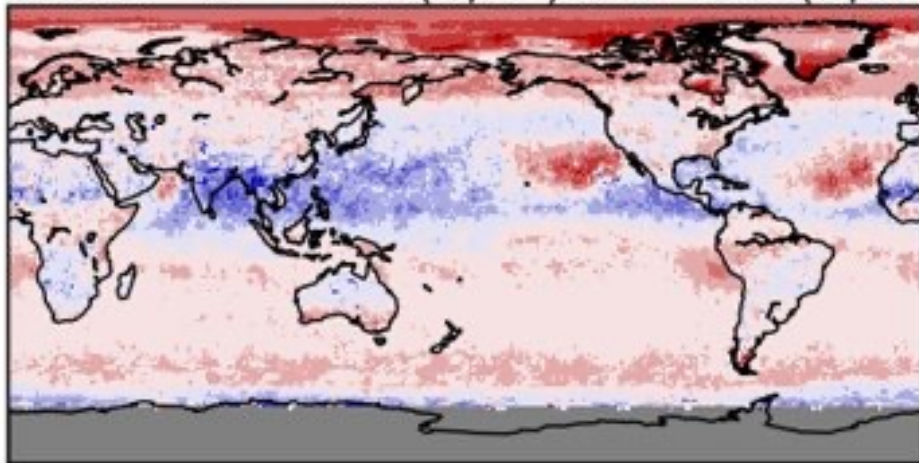
201601 $\Delta F = -1.36(w/m^2)$ rms= 2.28(w/m^2)



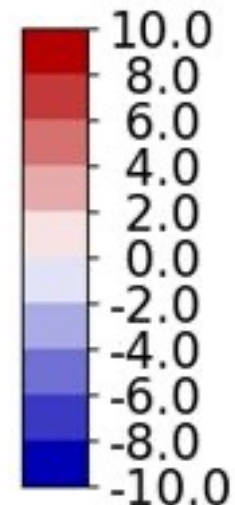
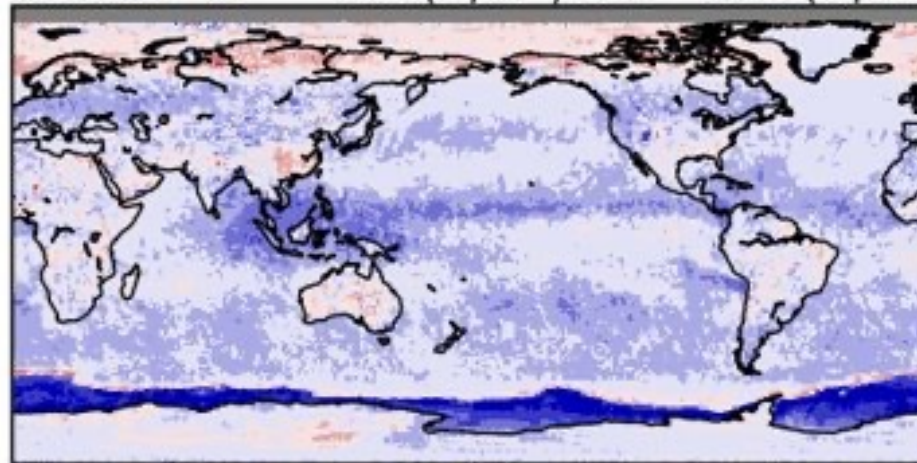
201604 $\Delta F = -1.72(w/m^2)$ rms= 2.49(w/m^2)



201607 $\Delta F = 0.65(w/m^2)$ rms= 2.26(w/m^2)



201610 $\Delta F = -1.78(w/m^2)$ rms= 2.55(w/m^2)



Direct Integration for SW Flux

- Construct two sets of regional ($10^\circ \times 10^\circ$) all-sky ADMs by season (e.g. DJF, MAM, JJA, and SON) from

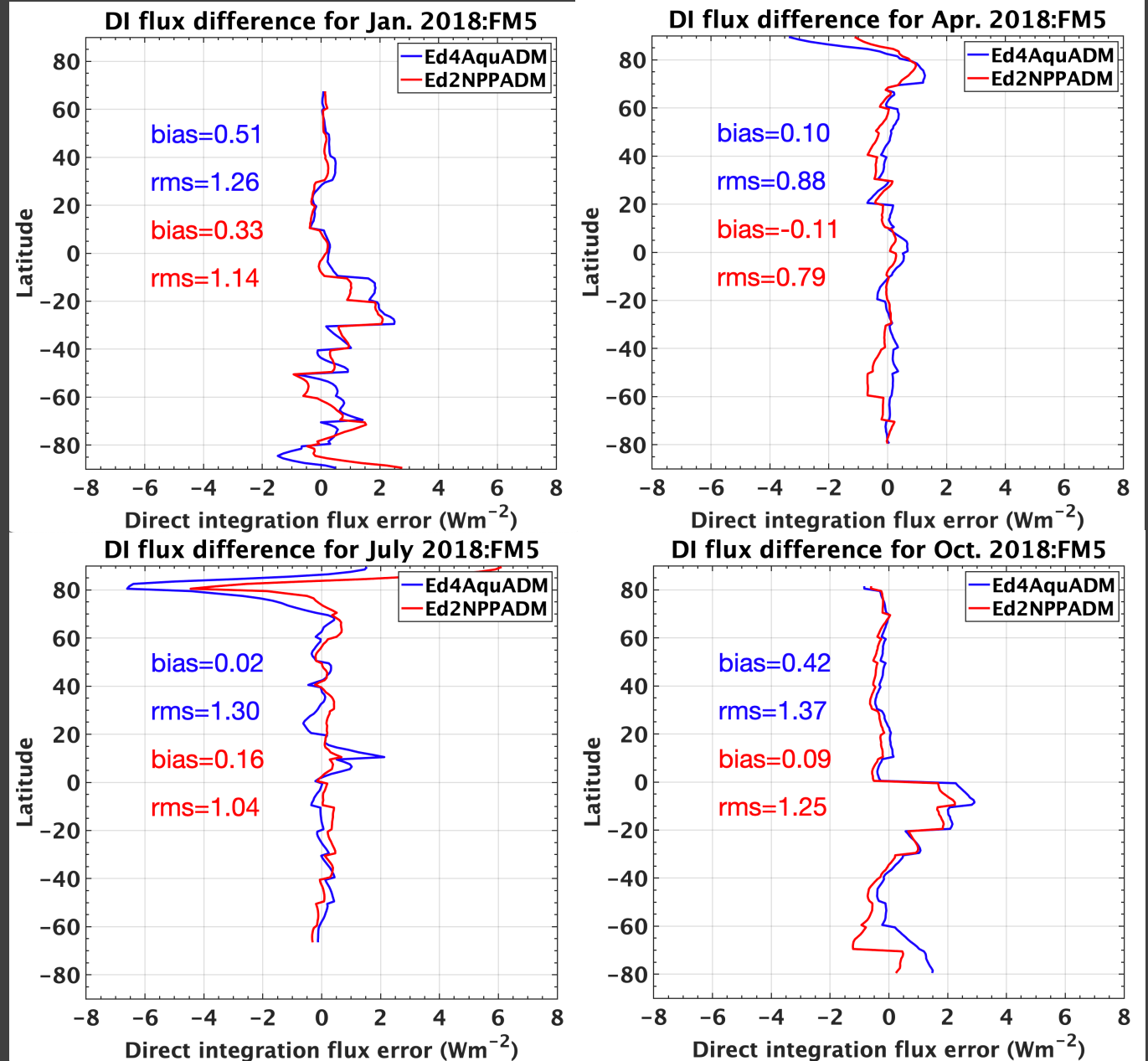
- CERES measured radiances $I_o \rightarrow F(\theta_0) = \frac{\pi I_o(\theta_0, \theta, \phi)}{R(\theta_0, \theta, \phi)}$

- ADM predicted radiances $\hat{I} \rightarrow R(\theta_0, \theta, \phi) = \frac{\pi \hat{I}(\theta_0, \theta, \phi)}{\hat{F}(\theta_0)}$

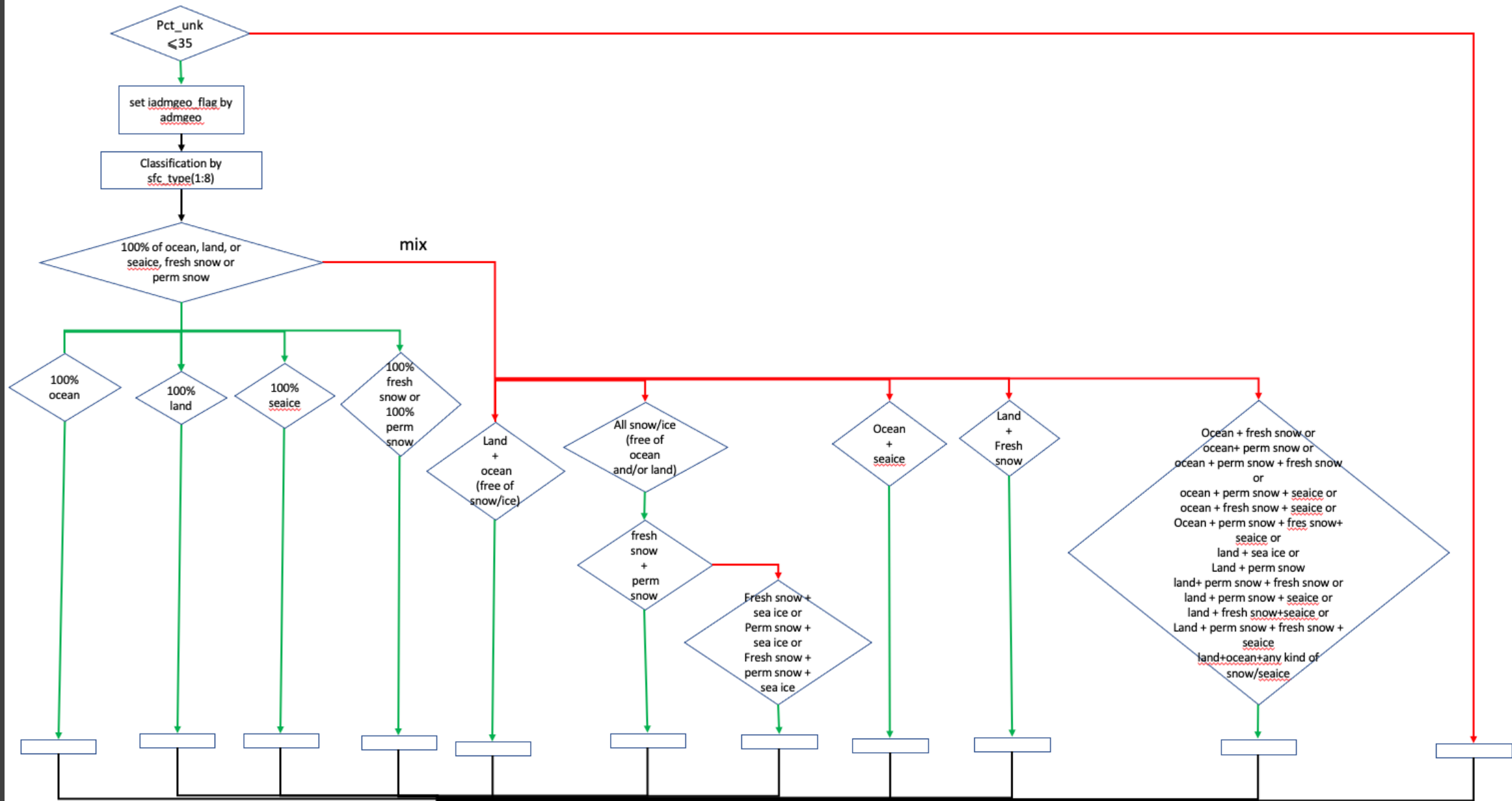
- Both sets of regional all-sky ADMs have the same sampling
- Apply regional ADMs to cross track data of the middle month of the season to determine the fluxes
- Compare fluxes derived from these two sets of ADMs

Direct integration SW flux error for 2018 NPP FM5

- Flux errors are defined as the flux difference inverted from predicted radiance ADM and from observed radiance ADM
- Zonal mean flux errors from NPP ADMs are generally smaller than those from Aqua ADMs
- Global mean flux errors from NPP ADMs are smaller than those from Aqua ADMs by about 10-20%

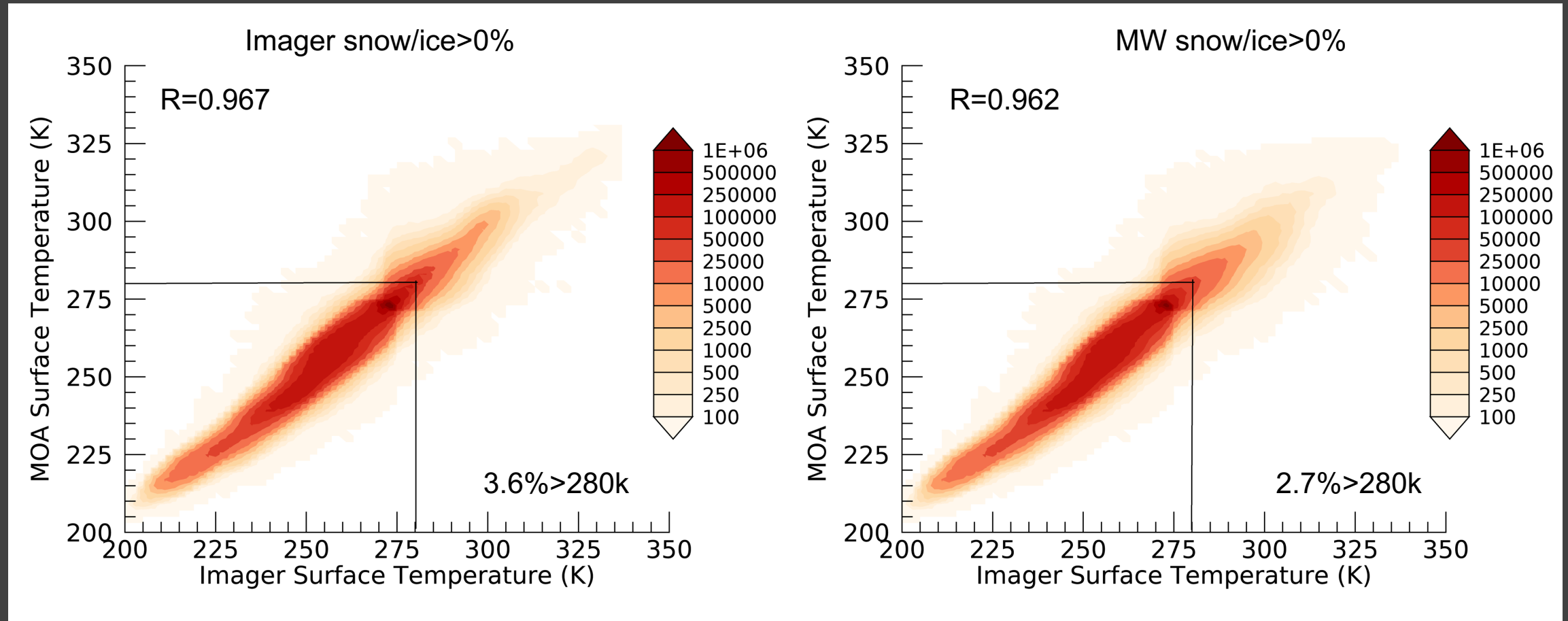


Rearchitect the shortwave inversion code



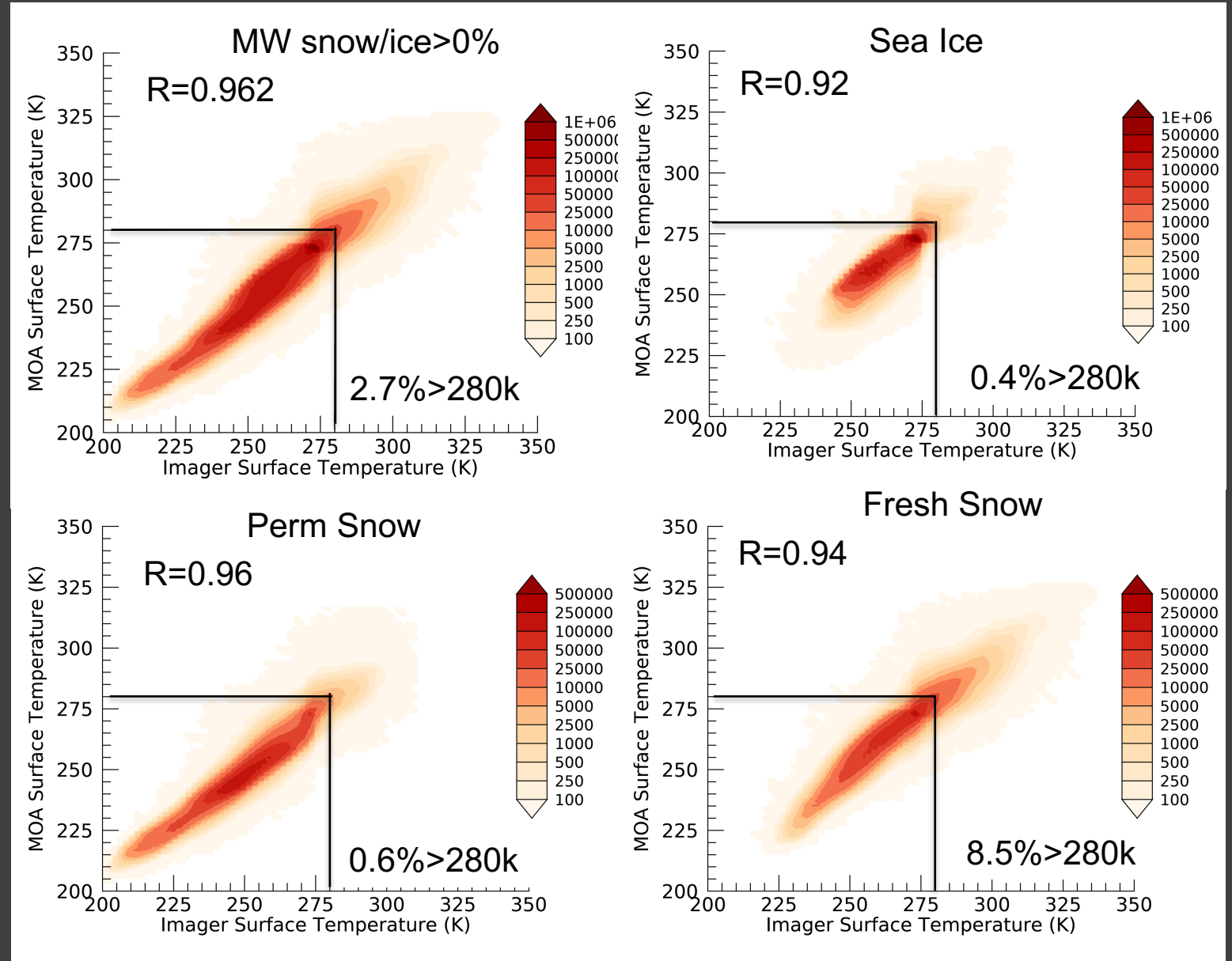
Snow ice variables used for inversion

- Scene identification relies on multiple variables, including imager- and microwave-based snow and ice fractions, and surface skin temperature from imager retrieval and reanalysis
- When imager- and microwave-based snow and ice information contradict each other, surface skin temperature is used to aid scene identification



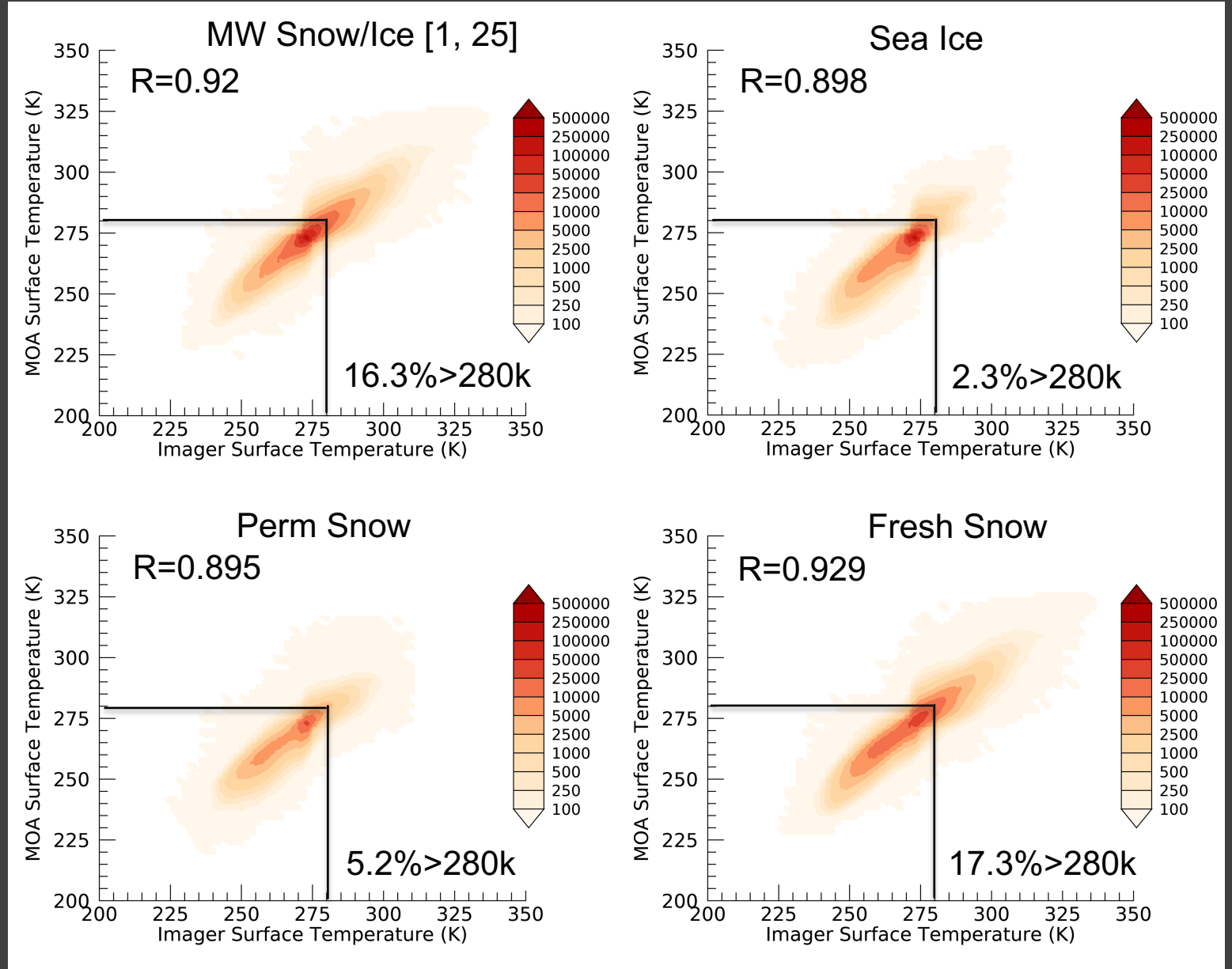
Percentage of snow/ice footprints with surface temperature > 280 K

- A small percentage of footprints that were identified as sea ice and permanent snow by microwave have a surface temperature greater than 280 K.
- A relatively large percentage of fresh snow footprints have surface temperature above 280 K.



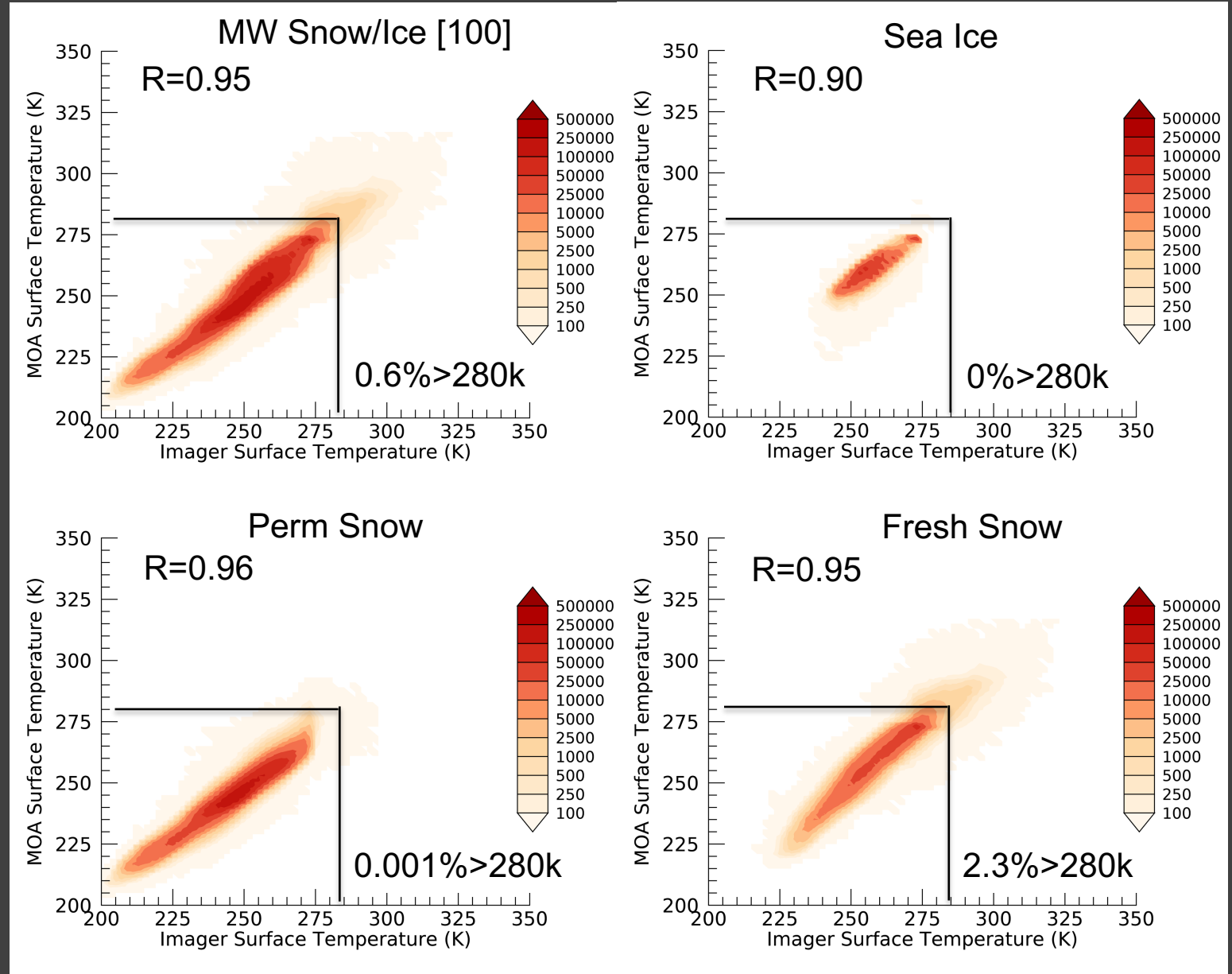
Footprints with partial snow/ice cover are more likely to have surface temperature >280 K

- For footprints with snow/ice fraction between 1 and 25%, large percentage of them have surface temperature exceeds 280 K, especially over fresh snow.



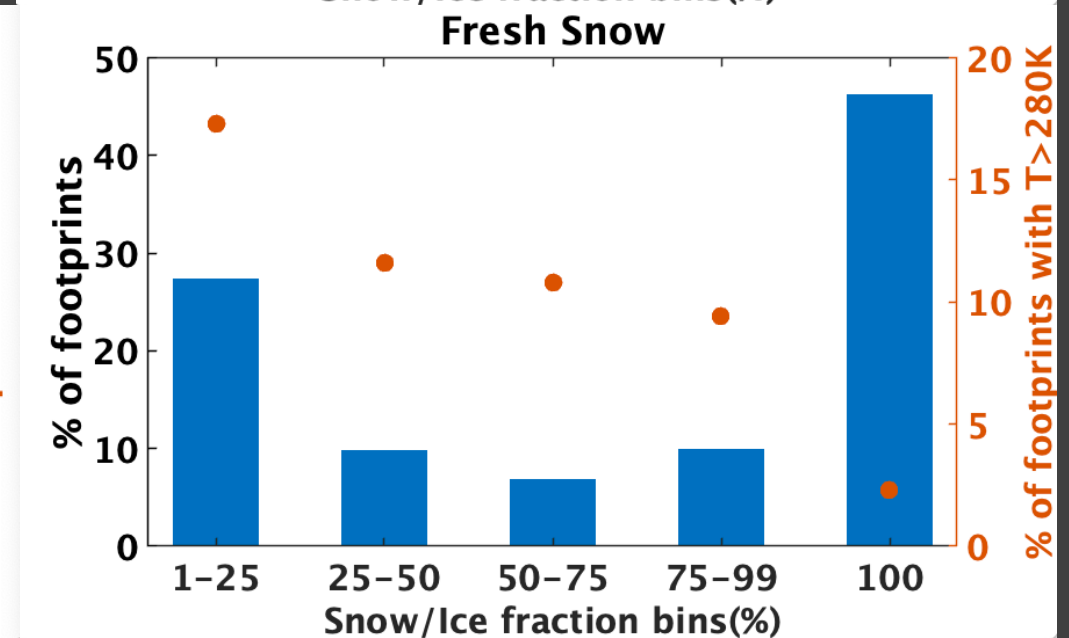
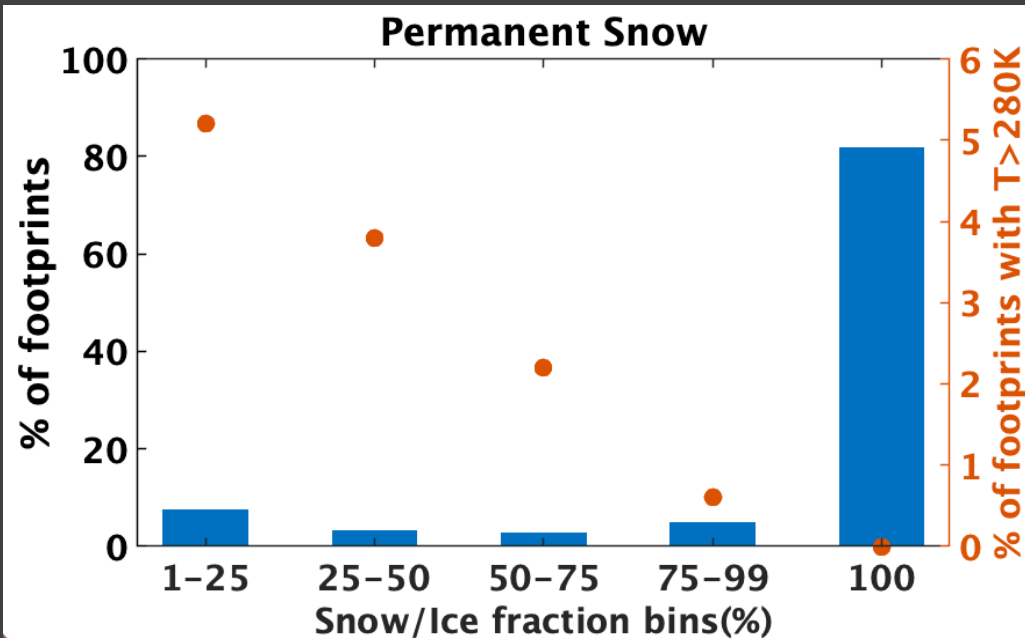
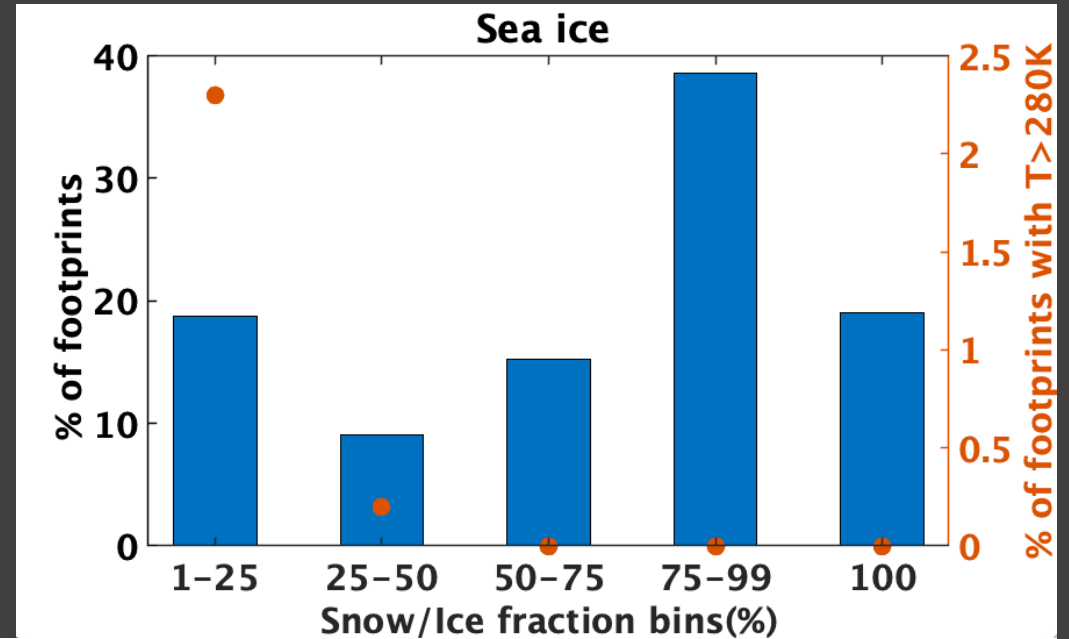
100% snow/ice footprints almost all have surface temperature <280 K

- For footprints with snow/ice fraction of 100%, large percentage of them have surface temperature exceeds 280 K, especially over fresh snow.



Large percentage of fresh snow footprints with $T > 280\text{K}$

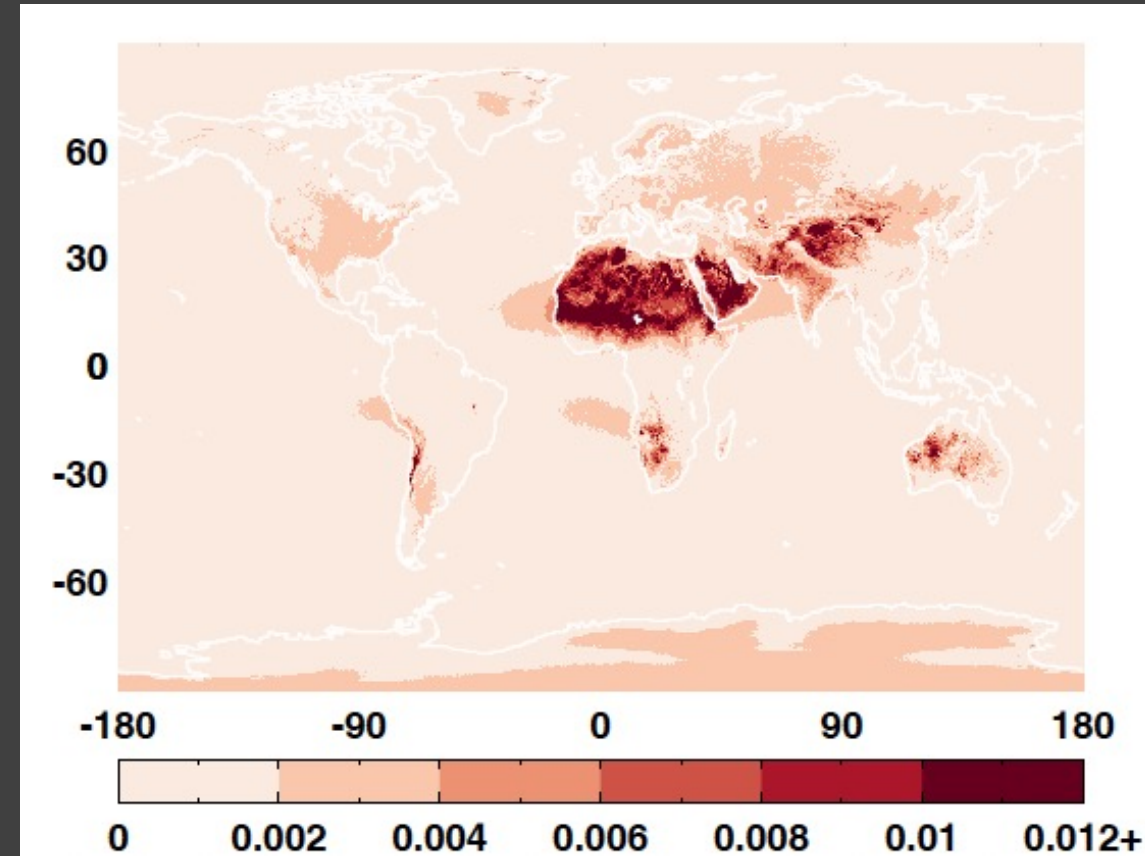
- For 100% snow/ice fractions, 280 K is a good threshold indicating that the temperature is too warm for snow/ice.
- For smaller snow/ice fractions, significant percentage of footprints (especially fresh snow) have temperature greater than 280 K.
- Temperature threshold will be reevaluated for Ed5 (possibly snow/ice fraction-based thresholds).



Surface emissivity

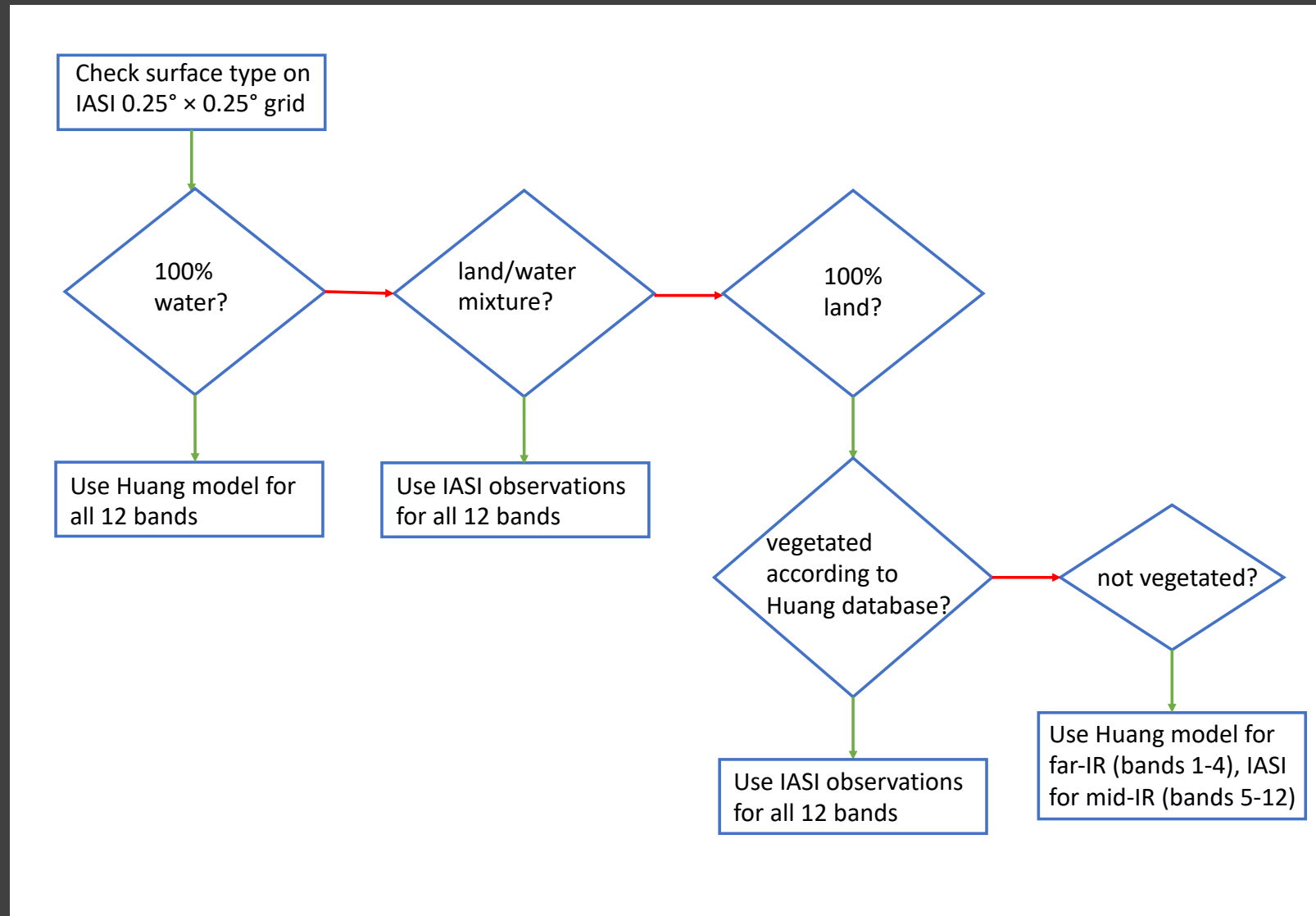
- The LW and WN emissivity is an input for the cloudy-sky LW ADMs.
- For Edition 4 and earlier editions, a single value of emissivity was assigned to each IGBP type for both the LW and WN channels.
- For Edition 5, a merged surface emissivity database is developed from IASI data and from theoretical calculation:
 - Monthly climatology of surface emissivity based on 10 years of IASI hyperspectral data between $3.62\ \mu\text{m}$ and $15.5\ \mu\text{m}$ (Zhou et al. 2011, 2013)
 - Theoretical calculation based on Fresnel equations and the spectrally dependent indices of refraction for water, snow/ice, and desert (Huang et al. 2016)

Range of monthly surface emissivity from IASI
Highest monthly – Lowest monthly emissivity



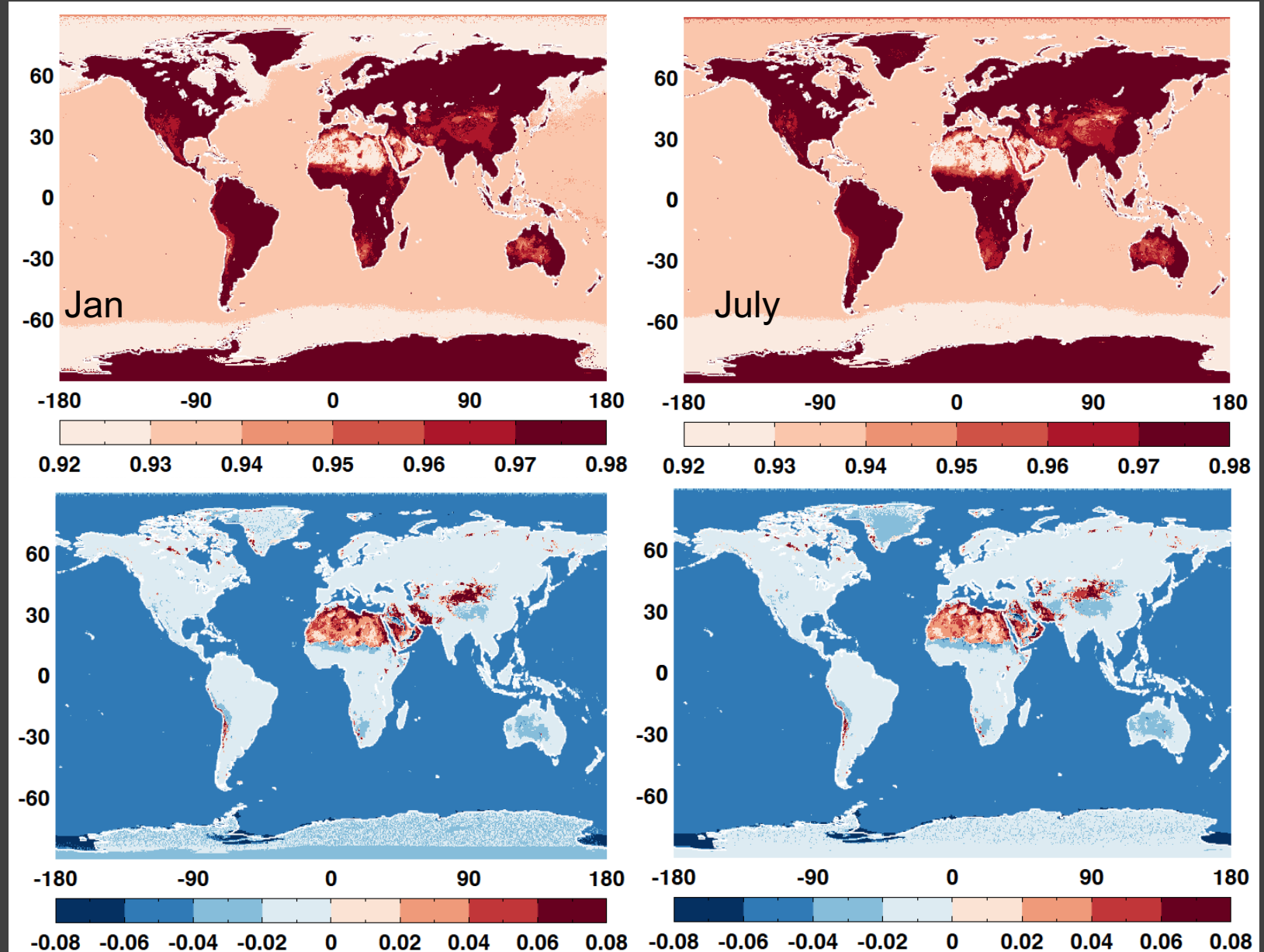
Merged monthly surface emissivity dataset

- Surface emissivity values for the 12 Fu-Liou bands
- They are weighted to provide the broadband LW and WN emissivity values
- The spatial resolution of the merged dataset is 0.25° by 0.25°



Emissivity difference between the merged dataset and the Ed.4 dataset

- Merged emissivity is significantly lower than that used in Edition 4 over water;
- Merged emissivity is slightly lower than that used in Edition 4 over most land areas;
- Merged emissivity is significantly higher than that used in Edition 4 over most desert regions.



Merged

Merged
-
Ed4

Summary

- Developed a set of NPP CERES SW ADMs based on NPP CERES cross track and RAPS data and the VIIRS cloud properties for scene identification.
- Global monthly mean instantaneous NPP SW fluxes inverted from NPP ADMs can differ from those inverted from Aqua ADMs by more than 1.5 Wm^{-2} , with the regional fluxes differing by up to 10 Wm^{-2} . Large regional differences are mostly over snow/ice surface due to significant cloud property differences between VIIRS and MODIS.
- Results from direct integration indicate that global mean flux errors from NPP ADMs are smaller than those from Aqua ADMs by about 10-20%.
- Merged monthly surface emissivity based on IASI and theoretical calculation will be used for CERES Ed 5 processing. Merged emissivity is significantly lower over water and is significantly higher over most desert regions than that used in Edition 4 .

Impact of surface emissivity on daytime LW flux inversion is small

- Bias is less than 0.1 Wm^{-2} .
- RMS is less than 1.2 Wm^{-2} .

